*Desalination and Water Treatment*
www.deswater.com

doi: 10.5004/dwt.2022.28531

261 (2022) 224–233
June

# Characterisation of activated carbons for removal of organic and heavy metal pollutants from water in resource limited countries

George Kalaba, James Nyirenda*, Onesmus Munyati

*Department of Chemistry, University of Zambia, P.O. Box: 32379, Lusaka, Zambia, emails: nyirendaj@unza.zm (J. Nyirenda), georgekalabajnr@gmail.com (G. Kalaba), omunyati@unza.zm (O. Munyati)*

Received 25 March 2021; Accepted 19 April 2022

**ABSTRACT**

Water contamination by heavy metals and organic waste presents a great challenge in developing countries, thereby hampering access to safe water. In this work, activated carbons were prepared from *Zea mays* cob (MC), *Anacardium occidentale* (cashew nut shells – CNS), sawdust from *Pinus oocarpa* (SPO) and *Pterocarpus angolensis* (SPA) biomass waste found in Zambia. The activated carbons were used as filters to remove heavy metals and organic pollutants from aqueous solution. The average adsorption efficiency of heavy metals was 99.10 ± 0.6%, 99.38 ± 0.4%, 98.43 ± 0.6% and 99.40 ± 0.4% for SPA, SPO, CNS and MC, respectively. Adsorption was found to follow Langmuir model for CNS and Freundlich model for SPA, SPO and MC. The adsorbent with high adsorption efficiency of heavy metals, MC was characterized using Fourier-transform infrared spectroscopy and further tested for methylene blue (MB) removal by adsorption. The kinetic data for adsorption of MB were best fitted by the pseudo-second-order kinetic model. The highest percentage removal of MB at equilibrium was 99.69 ± 0.3% at 50 mg/L and the lowest was 96.47 ± 0.1% at 350 mg/L indicating that maize cob activated carbon is an excellent adsorbent in the removal methylene blue and heavy metals even at low concentrations.

*Keywords:* Biomass; Activated carbon; Adsorption equilibrium; Isotherms; Kinetics

## 1. Introduction

The need for identification and fabrication of cheaper methods to remove heavy metals and organic pollutants from water is extremely critical in sub Saharan Africa. The increase in mining industries, agricultural activities, textile and abuse of water resources has contributed greatly to water contamination by heavy metals [1] and organic compounds such as paints [2], dyes [3], waste chemical effluents [4,5] and agrochemical residues [6]. Heavy metal pollution in many developing countries like Zambia includes high copper, zinc, cadmium and lead concentrations [7,8]. Accumulation of these metals in the human body can cause carcinogenesis, neurotoxicity, cell damage and loss of cellular functions [9,10]. The maximum permissible limit of cadmium, zinc, copper and lead in drinking water by World Health Organization are 0.003, 3, 2 and 0.01 mg/L, respectively [11]. Therefore, removal of these heavy metals from drinking water is a priority. Additionally, synthetic organic dyes are extremely essential in modern society as they add beauty and attractiveness to most products [12]. Nevertheless, dyes are considered to be among the most important water pollutants [13,14] as they are carcinogenic and causes many environmental problems [15–17]. The conventional techniques for removal of many pollutants from water includes; ion exchange process [18], chemical precipitation [19,20], ultra-filtration [21], electrodialysis [22], reverse osmosis process [23] and many others. These

* Corresponding author.

techniques are costly and requires high energy input [24,25]. On the other hand, adsorption has been widely utilized in practical operation due to its low operation cost, high efficiency and simplicity in operation [26,27]. Activated carbon is undoubtedly considered due to its exceptional high surface area, tuneable pore size and high adsorption capacity [28]. Waste biomass can be converted into activated carbon by physical and chemical processes [29]. Physical activation method is commonly used in many industries for production of activated carbon at a low cost because of lower activating agent price (steam and carbon dioxide) [29] and the activation process is easy to handle [28]. Nevertheless, controlling the textural characteristics of the activated carbon is difficult using physical activation method [28,29]. Unlike physical activation, chemical activation requires lower temperature and can be carried out in a single step, that is, thermal treatment of raw material with an activating agent such as $H_2SO_4$ [30], $H_3PO_4$ [31], $ZnCl_2$ [32], KOH [33,34] and NaOH [35], leading to the development of a more porous structure and of high surface area.

In the recent past, many studies have been conducted on the evaluation of low cost activated carbons from agricultural waste and some of them include; cashew nut shells [36], olive branches [37], honeydew peel [38], pistachio shells [39,40], olive stone waste [41], neem and mango bark [42] and many others. Although extensive research has been carried out on low cost agricultural waste adsorbent, few comparative studies of multiple low cost adsorbents exposed to the same conditions and at low metal ion concentrations have been carried out. Therefore, the present study was carried out to compare the adsorption efficiency of activated carbons prepared from *Anacardium occidentale* (cashew nut shells – CNS), *Zea mays* cob (MC), sawdust from two timber sources, *Pterocarpus angolensis* (SPA) and *Pinus oocarpa* (SPO) using sulphuric acid ($H_2SO_4$) activation [30]. Thereafter, batch adsorption experiments were carried out to compare the performance of the adsorbents for removal of Cu(II), Zn(II), Cd(II) and Pb(II) ions from water at very low metal ion concentrations. The adsorbent with high adsorption efficiency was characterised using Fourier-transform infrared spectroscopy (FT-IR) and further tested for adsorption of methylene blue (MB) by studying the effect of contact time, initial methylene blue concentration and kinetics.

## 2. Materials and methods

### 2.1. Materials

Cadmium nitrate tetrahydrate ($Cd(NO_3)_2{\cdot}4H_2O$), zinc nitrate hexahydrate ($Zn(NO_3)_2{\cdot}6H_2O$), copper(II) sulphate ($CuSO_4$), lead(II) nitrate ($Pb(NO_3)_2$), sulphuric acid 98%, methylene blue ($C_{16}H_{18}ClN_3S$) and distilled water.

Stock solutions of 1,000 mg/L metal ion concentrations were prepared by dissolving a specific mass of metal salt. Aqueous solutions of the standards were further prepared by serial dilution with distilled water. Methylene blue (MB) stock solutions were prepared by dissolving 1 g of MB made up to 1,000 mL solution from which other concentrations were prepared. All the reagents used in the experiments were of analytical grade.

### 2.2. Preparation of activated carbons from waste biomass

SPA and SPO saw dust shavings were washed severally with distilled water and dried at room temperature. Dry maize cobs (MC) were pulverized to 2 mm particle size. CNS were washed with distilled water and dried at room temperature and after size reduction, the cashew nut shell oil was extracted using solvent extraction. The raw materials were pre-heated at 110°C for 2 h in a Carbolite AAF 11/7 furnace at a heating rate of 10°C/min. Chemical activation with 50% sulphuric acid was carried out using an impregnation method [43,44]. The impregnation ratio of sulphuric acid to the raw materials were 2:1 [30]. Thus, 60 g of the preheated precursors were soaked in 86 mL of 50% sulphuric acid for 24 h. After soaking, the precursors were dried in an oven at 110°C. The dried precursors were carbonized in a Carbolite AAF 11/7 Furnace at 400°C for 3 h at a heating rate of 10°C /min. The carbonized products were cooled to room temperature and washed severally with hot distilled water until the pH was neutral. Thereafter, the cooled carbonized samples were then dried in an oven for 4 h, grounded and sieved using a 0.5 mm sieve. The activated carbons were stored in airtight bottles until use.

### 2.3. Adsorption experiments

Batch adsorption experiments were carried out to determine an adsorbent with higher percentage removal of Zn(II), Cu(II), Cd(II) and Pb(II) ions from aqueous solution using prepared activated carbons. The initial concentration of metal ions was varied from 0.05 to 3 mg/L whilst other parameters (1 g AC, pH = 6.98, temp. = 25°C and pressure = 1 atm) were kept constant. Thus, 1 g of each activated carbon was added to 30 mL of initial metal ion concentrations and the solution was agitated by shaking for 60 min at 250 rpm. Methylene blue adsorption was carried out using 1 g of activated carbon and 30 mL of MB and agitated at 250 rpm. All the experiments were carried out at 25°C and 1 atm. Heavy metal concentrations (initial and after adsorption) were measured on a Perkin Elmer AAnalyst 400 Atomic Absorption Spectrophotometer with detection limit of 0.002, 0.03, 0.01 and 0.02 mg/L for Cd, Cu, Pb and Zn, respectively (PerkinElmer, Inc., 940 Winter Street, Waltham, MA 02451 USA). A Shimadzu UV-2600 Spectrometer was used to determine the concentration of methylene blue standard before and after adsorption. Fig. 1 shows the calibration curve for MB adsorption.

Adsorption percentage (%) and the amount of adsorbate per unit mass of activated carbon ($q_e$) [36,45] was calculated using Eqs. (1) and (2).

$$\%\ \text{Adsorption} = \frac{\left(C_0 - C_e\right)\times 100}{C_0} \tag{1}$$

$$q_e = \frac{\left(C_0 - C_e\right)\times V}{m} \tag{2}$$

where $C_0$ is the initial concentration of adsorbate (mg/L), $C_e$ is the final concentration of adsorbate after adsorption (mg/L), $q_e$ is the amount of adsorbate adsorbed at equilibrium (mg/g), $m$ is the mass of activated carbon used (g) and $V$ is the volume of adsorbate solution used (mL).

### 2.4. Adsorption isotherm models

Three commonly models used to fit adsorption experiment results are the Langmuir, Freundlich and Temkin adsorption isotherm models [45,46].

#### 2.4.1. Langmuir isotherm model

The isotherm assumes that, the monolayer adsorption process happens between the adsorbate and homogenous surface of the adsorbent [47–49]. The binding sites have the same affinity for adsorption [50]. The linear equation is given below:

$$\frac{C_e}{q_e} = \frac{1}{K_L q_{\max}} + \frac{C_e}{q_{\max}} \tag{3}$$

where $q_e$ is the metal ions adsorbed (mg/g) at equilibrium, $C_e$ is the equilibrium concentration (mg/L), $q_{\max}$ is the monolayer adsorption capacity (mg/g) and $K_L$ is the Langmuir adsorption constant which is related to the energy of adsorption and is a measure of the metal ions affinity to the adsorption sites. The higher the magnitude of $K_L$ the more affinity between the adsorbent and the adsorbate molecules while a smaller value indicates a weak interaction [51,52]. The Langmuir parameters $q_{\max}$ and $K_L$ were calculated from the slope ($1/q_{\max}$) and intercept ($1/q_{\max}K_L$) of the plot of $C_e/q_e$ vs. $C_e$. An important characteristic of the Langmuir isotherm can be expressed in terms of the dimensionless equilibrium parameter or the separation factor, $R_L$ [53,54], which is defined as:

$$R_L = \frac{1}{1 + K_L C_0} \tag{4}$$

where $K_L$ is the Langmuir adsorption constant and $C_0$ is the initial metal ion concentration. The value of the separation factor gives an indication of the shape of the isotherm and the nature of the adsorption process. The values of the $R_L$ between 0 and 1 indicates favourable adsorption, unfavourable adsorption occurs when $R_L$ is greater than 1 and adsorption is linear when $R_L$ is equal to 1 [55].

#### 2.4.2. Freundlich isotherm model

The Freundlich isotherm model is an empirical model that explains that adsorption occurs on an unevenly distributed or heterogeneous surface of the adsorbent [56,57]. The adsorbent surface has different affinity and energy for adsorption [58]. Stronger binding sites are occupied first and then the binding strength decreases with the rise in the degree of site occupation. It is represented by the equation below:

$$\log q_e = \frac{1}{n}\left(\log C_e\right) + \log K_F \tag{5}$$

where $q_e$ is the metal ions adsorbed at equilibrium (mg/g), $C_e$ is the equilibrium concentration (mg/L), and $K_F$ is the Freundlich constant and $n$ is the adsorption intensity. The value of $n$ indicates the degree of non-linearity between metal ions concentration and its adsorption in the following manner; if $n$ is equal to 1 ($n$ = 1) then adsorption is linear, adsorption becomes a favourable physical process when $n$ is greater than 1 ($n$ > 1) and when $n$ is less than 1 ($n$ < 1) then adsorption is a chemical process [36,46]. From the slope ($1/n$) and intercept ($\log K_F$) of the plot of $\log q_e$ vs. $\log C_e$, the constant $K_F$ and $n$ can be calculated. Fig. 2 shows the Fourier-transform infrared spectrum of the raw and activated carbons between 4,000 and 400 cm$^{-1}$.

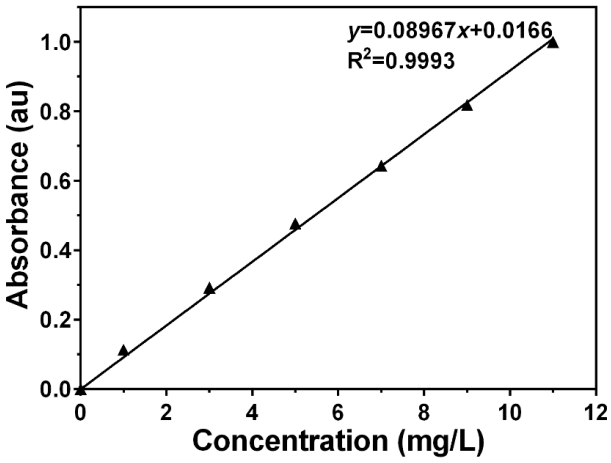


Fig. 1. Calibration curve for MB adsorption.

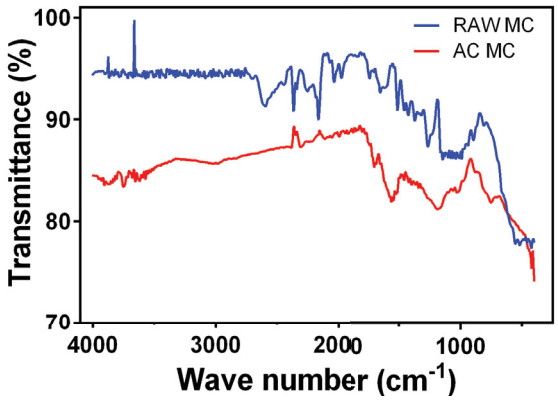


Fig. 2. FT-IR spectrum of maize cob activated carbon (MC-AC).

#### 2.4.3. Temkin isotherm model

The Temkin isotherm model considers the effect of indirect adsorbate–adsorbent interaction on the adsorption process [59,60]. It is based on the assumption that the heat of adsorption of all the molecules in a layer decreases linearly due to increase in surface coverage of the adsorbent [61–63]. The decrease in heat of adsorption is linear rather than logarithmic, as implied in the Freundlich isotherm. Further, the adsorption is characterized by uniform distribution of binding energies, up to a maximum binding energy. The Temkin isotherm model is represented by the following equation [45]:

$$q_e = \frac{RT}{b}\ln K_T + \frac{RT}{b}\ln C_e \quad (6)$$

where $K_T$ is the equilibrium binding constant (L/mol) corresponding to the maximum binding energy, $b$ is related to the adsorption heat, $R$ is the universal gas constant (8.314 J/K mol) and $T$ is the temperature at 298 K. The constants $K_T$ and $b$ can be calculated from the slope ($RT/b$) and intercept ($RT\ln K_T/b$) of the plot of $q_e$ vs. $\ln(C_e)$ [45].

## 3. Results and discussion

In order to assess the use of biomass-derived activated carbon from various types of waste generated in various processes of Zambia as low cost sources of filtration material, two experiments were set up to model removal of heavy metals and dyes from waste water. Batch adsorption was carried out for the removal of Cu(II), Pb(II), Cd(II) and Zn(II) using SPA, SPO, CNS and MC adsorbate. The average percentage removal was 99.10 ± 0.6%, 99.38 ± 0.4%, 98.43 ± 0.6% and 99.40 ± 0.4% for SPA, SPO, CNS and MC respectively. Overall, activated carbon from maize cob had slightly the highest average removal percentage for the metal ions and the least was activated carbon from cashew nut shells as shown in Table 1. Nevertheless, SPO was a better adsorbent for lead (Pb) ions at 99.50 ± 0.3% followed by MC at 99.40 ± 0.7%, SPA and MC had the highest removal percentage for zinc (Zn) and cadmium (Cd) ions respectively. The highest removal percentage of copper (Cu) ions was 99.40% by SPO and CNS.

Table 1 shows the percent removal of heavy metals from aqueous solution at 25°C. Overall, MC, SPO, SPA and CNS showed a higher removal capacity at 99.4 ± 0.4%, 99.38 ± 0.4%, 99.1 ± 0.6% and 98.43 ± 0.6%, respectively.

### 3.1. Adsorption isotherms

#### 3.1.1. Langmuir isotherm model

The Langmuir parameters of Cu(II), Pb(II), Cd(II) and Zn(II) using SPA, SPO, CNS and MC were obtained from the plot of $C_e/q_e$ vs. $C_e$ and using Eq. (4). The correlation coefficient ($R^2$), $q_{max}$, $K_L$ and $R_L$ are summarized in Tables 2–5. The regression correlation coefficient was highest for the removal of Cu(II), Pb(II), Cd(II) and Zn(II) using CNS. Thus, adsorption of heavy metals using CNS followed Langmuir adsorption isotherm. The finding that CNS followed Langmuir isotherm was supported by [64] but was also contrary to the finding by [65] whose isotherm followed Freundlich isotherm. The differences in isotherms can be attributed to the differences in activation of CNS biomass and the functional groups present on the activated carbon. Thus, adsorption of heavy metals onto CNS was monolayer and the binding sites had equal affinity for adsorption [66–68]. The higher magnitude of $K_L$ suggested a high affinity between the adsorbent and the metal ions [30]. The estimated minimum and maximum $R_L$ ranged from 0.0003 to 0.881, which indicated favourable adsorption [69–71]. The adsorption capacities were low for all the adsorbents, this is because the adsorption capacity of any adsorbent increases with increasing metal ion concentration [72] and the concentrations of metal ions used were very low (0.05–3 mg/L). Also, the low adsorption capacity may be due to the high adsorbent amount (1 g) which leads to an increase in the number of active sites available for the adsorption process compared to the metal ions [73].

#### 3.1.2. Freundlich isotherm model

The Freundlich parameters $K_F$ and $n$ (Tables 2–5) were calculated from the slope and intercept of the plot of $\ln q_e$ against $\ln C_e$. The Freundlich regression correlation coefficient ($R^2$) values of Cu(II), Pb(II), Cd(II) and Zn(II) for SPA, SPO and MC were higher compared to those of Langmuir and Temkin isotherm models. Adsorption using SPA, SPO and MC followed Freundlich isotherm model. Therefore, heterogeneous adsorption of heavy metals on the surface of the adsorbents was predominant [74,75].

#### 3.1.3. Temkin isotherm model

The equilibrium experimental data was also fitted with the Temkin isotherm model. The Temkin adsorption parameters $b_T$ and $K_T$ were calculated from the plot of $q_e$ vs. $\ln C_e$ (Tables 2–5). The regression correlation coefficient ($R^2$) values obtained for Temkin isotherm model was less than that of Langmuir and Freundlich adsorption model. Thus, the isotherm couldn't be used to describe and fit the adsorption process [76].

Therefore, adsorption followed Langmuir model for CNS and Freundlich model for SPA, SPO and MC. Maize cob activated carbon (MC) exhibited a high adsorption efficiency and was used in the production of AC-Ag-$SiO_2$ composite.

Tables 2–5 show the data for the four heavy metals; Cu, Cd, Pb and Zn with respect to Langmuir, Freundlich and Temkin adsorption isotherms and the respective adsorbent.

Table 6 compares the adsorption efficiency of various activated carbons from different sources including the ones

Table 1
Adsorption efficiency of heavy metals onto the adsorbents

| Adsorbent | % Adsorption | | | | |
|---|---|---|---|---|---|
| | Cu | Pb | Cd | Zn | Average |
| SPA | 98.6 ± 1.1 | 98.7 ± 0.7 | 99.4 ± 0.4 | 99.7 ± 0.1 | 99.10 ± 0.6 |
| SPO | 99.4 ± 0.3 | 99.5 ± 0.3 | 99.3 ± 0.4 | 99.3 ± 0.6 | 99.38 ± 0.4 |
| CNS | 99.4 ± 0.5 | 95.4 ± 1.5 | 99.4 ± 0.2 | 99.5 ± 0.1 | 98.43 ± 0.6 |
| MC | 99.1 ± 0.5 | 99.4 ± 0.7 | 99.5 ± 0.3 | 99.6 ± 0.2 | 99.40 ± 0.4 |

Table 2
Langmuir, Freundlich and Temkin isotherm constants for the removal of Cu(II), Pb(II), Cd(II) and Zn(II) using SPA

| Metal | Langmuir | | | | Freundlich | | | Temkin | | |
|---|---|---|---|---|---|---|---|---|---|---|
| | $R^2$ | $q_{max}$ | $K_L$ | $R_L$ | $R^2$ | $K_F$ | $n$ | $R^2$ | $b_T$ | $K_T$ |
| Cu | 0.695 | 0.044 | 100.6 | 0.0003–0.33 | 0.969 | 0.0182 | –0.51 | 0.726 | –137,643 | 0.94 |
| Zn | 0.697 | 0.064 | 882.8 | 0.0004–0.36 | 0.865 | 0.0203 | –0.54 | 0.495 | –168,542 | 0.63 |
| Pb | 0.817 | 0.084 | 103.7 | 0.0032–0.82 | 0.964 | 0.0181 | –0.71 | 0.593 | –184,893 | 1.34 |
| Cd | 0.707 | 0.084 | 195.2 | 0.0017–0.72 | 0.919 | 0.0191 | –0.64 | 0.689 | –193,560 | 1.12 |

Table 3
Langmuir, Freundlich and Temkin isotherm constants for the removal of Cu(II), Pb(II), Cd(II) and Zn(II) using SPO

| Metal | Langmuir | | | | Freundlich | | | Temkin | | |
|---|---|---|---|---|---|---|---|---|---|---|
| | $R^2$ | $q_{max}$ | $K_L$ | $R_L$ | $R^2$ | $K_F$ | $n$ | $R^2$ | $b_T$ | $K_T$ |
| Cu | 0.749 | 0.081 | 214.3 | 0.0016–0.70 | 0.920 | 0.0190 | –0.62 | 0.776 | –134,650 | 1.01 |
| Zn | 0.989 | 0.099 | 316.3 | 0.0009–0.58 | 0.923 | 0.0190 | –0.68 | 0.492 | –165,171 | 0.65 |
| Pb | 0.866 | 0.065 | 801.3 | 0.0004–0.38 | 0.758 | 0.0233 | –0.80 | 0.587 | –184,893 | 0.75 |
| Cd | 0.679 | 0.055 | 972.3 | 0.0003–0.34 | 0.923 | 0.0178 | –0.62 | 0.699 | –195,084 | 0.90 |

Table 4
Langmuir, Freundlich and Temkin isotherm constants for the removal of Cu(II), Pb(II), Cd(II) and Zn(II) using CNS

| Metal | Langmuir | | | | Freundlich | | | Temkin | | |
|---|---|---|---|---|---|---|---|---|---|---|
| | $R^2$ | $q_{max}$ | $K_L$ | $R_L$ | $R^2$ | $K_F$ | $n$ | $R^2$ | $b_T$ | $K_T$ |
| Cu | 0.929 | 0.090 | 173.6 | 0.0019–0.74 | 0.831 | 0.0212 | –0.65 | 0.450 | –208,199 | 0.51 |
| Zn | 0.995 | 0.089 | 597.7 | 0.0006–0.46 | 0.510 | 0.0494 | –3.34 | 0.411 | –196,632 | 0.48 |
| Pb | 0.874 | 0.089 | 67.30 | 0.0049–0.88 | 0.751 | 0.0235 | –0.88 | 0.513 | –203,079 | 0.61 |
| Cd | 0.873 | 0.090 | 199.5 | 0.0017–0.72 | 0.909 | 0.0201 | –0.56 | 0.356 | –302,142 | 0.26 |

Table 5
Langmuir, Freundlich and Temkin isotherm constants for the removal of Cu(II), Pb(II), Cd(II) and Zn(II) using MC

| Metal | Langmuir | | | | Freundlich | | | Temkin | | |
|---|---|---|---|---|---|---|---|---|---|---|
| | $R^2$ | $q_{max}$ | $K_L$ | $R_L$ | $R^2$ | $K_F$ | $n$ | $R^2$ | $b_T$ | $K_T$ |
| Cu | 0.838 | 0.077 | 192.7 | 0.002–0.722 | 0.870 | 0.0202 | –0.60 | 0.511 | –182,174 | 0.64 |
| Zn | 0.813 | 0.075 | 455.1 | 0.0007–0.52 | 0.732 | 0.0241 | –0.89 | 0.330 | –313,616 | 0.22 |
| Pb | 0.995 | 0.089 | 535.0 | 0.0006–0.48 | 0.920 | 0.0190 | –0.68 | 0.606 | –184,893 | 0.77 |
| Cd | 0.762 | 0.077 | 309.2 | 0.0011–0.62 | 0.927 | 0.0188 | –0.65 | 0.606 | –193,560 | 0.76 |

from SPA and SPO, some of the bulky waste biomass in Zambia derived from the timber and saw milling industries.

### *3.2. Study of the adsorption kinetics of methylene blue using maize cob activated carbon*

#### *3.2.1. Characterization of maize cob activated carbon using FT-IR*

The FT-IR analysis of activated maize cob confirms a band at around 3,010 $cm^{-1}$ which can be assigned to O–H stretching vibration of carboxylic group [81], the band at 1,784 $cm^{-1}$ relates to C=O stretching of carboxylic group [82], The band at 1,556 $cm^{-1}$ confirms the presence of C=C stretching vibration in aromatic rings [82,83], the band around 1,185 $cm^{-1}$ can be assigned to C–O or C–O–C stretching vibrations [84]. Thus, the presence of O–H and C=O bands suggests that the maize cob was activated by sulphuric acid.

#### *3.2.2. Effect of contact time and initial methylene blue concentration*

The study of effect of contact time is significant in calculating kinetic parameters and in the determination of

Table 6
Comparison of adsorption efficiency for various adsorbents

| Adsorbent | Adsorption efficiency (%) | | | | References |
|---|---|---|---|---|---|
| | Cu(II) | Pb(II) | Cd(II) | Zn(II) | |
| SPA | 98.6 ± 1.1 | 98.7 ± 0.7 | 99.4 ± 0.4 | 99.7 ± 0.1 | This work |
| SPO | 99.4 ± 0.3 | 99.5 ± 0.3 | 99.3 ± 0.4 | 99.3 ± 0.6 | This work |
| CNS | 99.4 ± 0.5 | 95.4 ± 1.5 | 99.4 ± 0.2 | 99.5 ± 0.1 | This work |
| MC | 99.1 ± 0.5 | 99.4 ± 0.7 | 99.5 ± 0.3 | 99.6 ± 0.2 | This work |
| OSAC | 99.24 | 99.32 | – | – | [41] |
| Corn cob | – | – | 93.63 | – | [77] |
| African palm tree | 96.71 ± 0.08 | 97.75 ± 0.17 | 99.24 ± 0.15 | – | [78] |
| Sugarcane bagasse | 90 | 99.9 | – | – | [79] |
| Coconut shell | – | – | 83.7 | – | [80] |
| Melanin AC | 93.8 | 91.1 | – | – | [66] |

the rate and kinetic behaviour of the adsorption process [85]. Thus, the effect of contact time and initial concentration on adsorption of MB on maize cob activated carbon were carried out using 30 mL solution of initial MB concentration of 50, 150, 250 and 350 mg/L at different time intervals. The experimental results of adsorption of MB at different initial concentrations and time are shown in Fig. 3. The percentage removal of MB increased as contact time increased until equilibrium was achieved at 180, 160, 140 and 100 min for 350, 250, 150 and 50 mg/L, respectively. This trend is in agreement with the results obtained by [86–88]. Also, the percentage removal of MB decreased from 99.69 ± 0.3% to 96.47 ± 0.1% as initial MB concentration increased from 50 to 350 mg/L and the results are supported by [89,90].

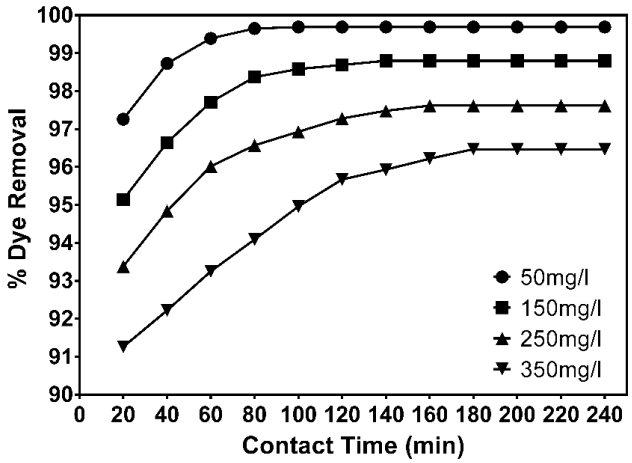


Fig. 3. Effect of contact time and initial concentration on MB adsorption. The graph was plotted using GraphPad Prism version 6.01. Fitting was done by using the points and connection option.

### 3.2.3. Adsorption kinetic models

The adsorption kinetic models are important in evaluating the rate and kinetic behaviour of the adsorption process. The kinetic parameters provide substantial information in designing and modelling of the adsorption process [91]. The kinetic of methylene blue (MB) adsorption onto maize cob activated carbon was analysed using pseudo-first-order and pseudo-second-order kinetic models.

A pseudo-first-order kinetic equation is given as [30,41]:

$$\log\left(q_e - q_t\right) = \log q_e - \frac{K_1}{2.303}t \tag{7}$$

where $q_e$ and $q_t$ (mg/g) are the amounts of methylene blue (MB) adsorbed at equilibrium and at time $t$ (min), $K_1$ (min$^{-1}$) is the adsorption rate constant. The parameters $q_e$ and $K_1$ were determined from the intercept and slope of a plots of $\log(q_e - q_t)$ vs. $t$ as shown in Fig. 4. The parameters of pseudo-first-order kinetic are tabulated in Table 7.

Pseudo-second-order kinetic model is expressed as [92];

$$\frac{t}{q_t} = \frac{1}{K_2 q_e^2} + \frac{1}{q_e}t \tag{8}$$

where $K_2$ (g/mg min) is second-order adsorption rate constant, $h$ (mg/g min) is the initial adsorption rate.

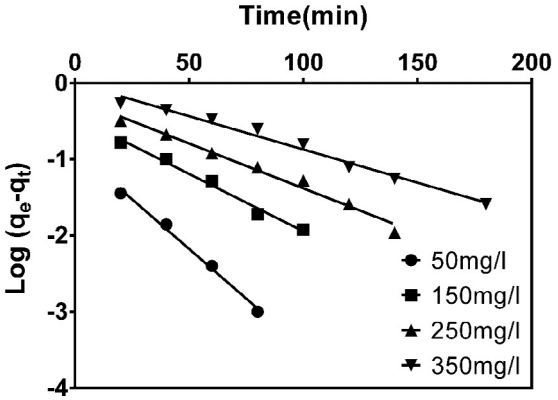


Fig. 4. Pseudo-first-order adsorption kinetics of MB. The graphs were plotted using GraphPad Prism version 6.01. Fitting was done using the linear regression mode with $R^2$ value being 0.9931, 0.9858, 0.9821 and 0.9813 for the 50, 150, 250 and 350 mg/L adsorption, respectively.

Table 7
Pseudo-first-order and pseudo-second-order kinetic models for the adsorption of methylene blue (MB) onto maize cob activated carbon

| Kinetic parameter | Initial concentration (mg/L) | | | |
|---|---|---|---|---|
| | 50 | 150 | 250 | 350 |
| $q_{e,exp}$ (mg/g) | 1.495 | 4.448 | 7.322 | 10.129 |
| Pseudo-first-order kinetic | | | | |
| $R^2$ | 0.9931 | 0.9858 | 0.9921 | 0.9813 |
| $q_{e,cal}$ (mg/g) | 0.135 | 0.365 | 0.626 | 0.991 |
| $K_1$ | 0.006 | 0.035 | 0.027 | 0.02 |
| Pseudo-second-order kinetic | | | | |
| $R^2$ | 1 | 1 | 1 | 0.9874 |
| $q_{e,cal}$ (mg/g) | 1.507 | 4.482 | 7.375 | 11.211 |
| $K_2$ | 1.004 | 0.205 | 0.101 | 0.01 |

The parameters $q_e$ and $K_2$ were calculated from the slope and intercept of the plots of $t/q_t$ vs. $t$ as shown in Fig. 5.

Pseudo-first-order and pseudo-second-order kinetic parameters for different initial concentrations of methylene blue are tabulated in Table 7. The value of the correlation coefficient ($R^2$) for pseudo-second-order model is higher than the value of pseudo-first-order adsorption model. Furthermore, pseudo-second-order model has values of $q_{e,cal}$ which are close to $q_{e,exp}$. It can be concluded that the adsorption of methylene blue onto maize cob activated carbon follows pseudo-second-order kinetic model. The results are in agreement with the results obtained by [93,94]. This implies that, the rate-limiting step is the surface adsorption that involves chemical adsorption with the polar functional group (carboxylic acid) present on activated MC which acts as a chemical bonding agent. Thus, chemical adsorption likely occurs through the formation of a covalent bond.

Table 7 shows the kinetics for maize cob activated carbon and adsorption of methylene blue dye. The pseudo-second-order kinetics fitted well with the experimental data.

The kinetic data were best fitted by the pseudo-second-order kinetic model. The obtained results for adsorption kinetics were rather inconsistent with Jawad et al. [82] but were in agreement with [93,94] presenting an opportunity to further study the adsorption kinetics of maize cob activated carbon.

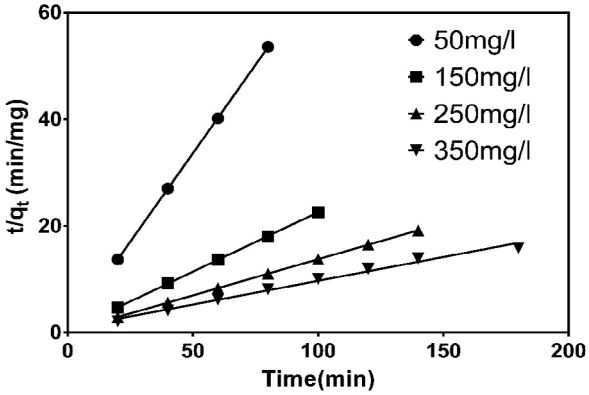


Fig. 5. Pseudo-second-order adsorption kinetics of MB. The graphs were plotted using GraphPad Prism version 6.01. Fitting was done using the linear regression mode with $R^2$ value being 1.000, 1.000, 1.000 and 0.9874 for the 50, 150, 250 and 350 mg/L adsorption, respectively.

## 4. Conclusion

Activated carbons from maize cob, cashew nut shells, *Pinus oocarpa* and *Pterocarpus angolensis* saw dust were prepared using sulphuric acid activation and used for removal of Cu, Pb, Cd and Zn ions from aqueous solution. The percentage removal was 99.10 ± 0.6%, 99.38 ± 0.4%, 98.4 ± 0.6% and 99.40 ± 0.4% for SPA, SPO, CNS and MC respectively. Activated carbon from MC had a slight high percentage removal compared with the other activated carbons. Adsorption followed the Langmuir model for CNS and Freundlich model for SPA, SPO and MC. Based on the results obtained, the prepared activated carbons have the potential to be used as filters in removing Cu, Pb, Cd and Zn ions from water. The highest percentage removal of MB at equilibrium was 99.69 ± 0.3% at 50 mg/L and the lowest was 96.47 ± 0.1% at 350 mg/L indicating that maize cob activated carbon is an excellent adsorbent in the removal of methylene blue and heavy metals even at low concentrations.

## Competing interests

The authors declare that they have no competing interests.

## Funding

This research did not receive any specific grant from funding agencies in the public, commercial, or not-for-profit sectors.

## Author contribution

JN, conceptualized the study, GK and JN carried out sample collection. JN and OM designed the experiments. GK carried out the experiments. JN and GK wrote the paper. OM read the paper. All authors read and contributed to editing.

## Acknowledgements

The authors would like to thank members of the Departments of Chemistry-School of Natural Sciences, Technology Development Advisory Unit-School of Engineering of the University of Zambia for the equipment and services rendered. Gratitude also goes to the International Programme in the Chemical Sciences at Uppsala University, Sweden, for the indirect support received during the execution of the research.

## References

[1] M.N. Chileshe, S. Syampungani, E.S. Festin, M. Tigabu, A. Daneshvar, P.C. Odén, Physico-chemical characteristics and heavy metal concentrations of copper mine wastes in Zambia: implications for pollution risk and restoration, J. For. Res., 31 (2020) 1283–1293.
[2] T.E. Aniyikaiye, T. Oluseyi, J.O. Odiyo, J.N. Edokpayi, Physico-chemical analysis of wastewater discharge from selected paint industries in Lagos, Nigeria, Int. J. Environ. Res. Public Health, 16 (2019) 1235, doi: 10.3390/ijerph16071235.
[3] G.K. Weldegebrieal, Synthesis method, antibacterial and photocatalytic activity of ZnO nanoparticles for azo dyes in wastewater treatment: a review, Inorg. Chem. Commun., 120 (2020) 108140, doi: 10.1016/j.inoche.2020.108140.
[4] K.M. Namwanja, S.M. Siachoono, A.M. Yambayamba, L. Chama, The impact of mine effluents on the water quality and macrophyte plant communities in the Kifubwa Stream, Solwezi, Zambia, Nat. Resour., 9 (2018) 198–211.
[5] E. Ngumba, A. Gachanja, J. Nyirenda, J. Maldonado, T. Tuhkanen, Occurrence of antibiotics and antiretroviral drugs in source-separated urine, groundwater, surface water and wastewater in the peri-urban area of Chunga in Lusaka, Zambia, Water SA, 46 (2020) 278–284.
[6] E. Lema, R. Machunda, K.N. Njau, Agrochemicals use in horticulture industry in Tanzania and their potential impact to water resources, Int. J. Biol. Chem. Sci., 8 (2014) 831–842.
[7] Y. Ikenaka, S.M. Nakayama, K. Muzandu, K. Choongo, H. Teraoka, N. Mizuno, M. Ishizuka, Heavy metal contamination of soil and sediment in Zambia, Afr. J. Environ. Sci. Technol., 4 (2010) 729–739.
[8] G.N. Ngweme, E.K. Atibu, D.M.M. Al Salah, P.M. Muanamoki, G.M. Kiyombo, C.K. Mulaji, J.-P. Otamonga, J.W. Poté, Heavy metal concentration in irrigation water, soil and dietary risk assessment of *Amaranthus viridis* grown in peri-urban areas in Kinshasa, Democratic Republic of the Congo, Watershed Ecol. Environ., 2 (2020) 16–24.
[9] G.A. Engwa, P.U. Ferdinand, F.N. Nwalo, M.N. Unachukwu, Mechanism and Health Effects of Heavy Metal Toxicity in Humans, O. Karcioglu, B. Arslan, Eds., Poisoning in the Modern World-New Tricks for an Old Dog?, IntechOpen, 2019, pp. 1–23.
[10] P.B. Tchounwou, C.G. Yedjou, A.K. Patlolla, D.J. Sutton, Heavy metals toxicity and the environment, EXS, 101 (2012) 133–164.
[11] WHO, Guidelines for Drinking-Water Quality, WHO Chronicle, 38 (2011) 104–108.
[12] E.A. Clarke, R. Anliker, Organic Dyes and Pigments, In: Anthropogenic Compounds, The Handbook of Environmental Chemistry, Vol. 3/3A, Springer, Berlin, Heidelberg, 1980, pp. 181–215.
[13] Q. Feng, H. Cheng, F. Chen, X. Zhou, P. Wang, Y. Xie, Investigation of cationic dye adsorption from water onto acetic acid lignin, J. Wood Chem. Technol., 36 (2016) 173–181.
[14] Z. Sun, K. Qu, Y. Cheng, Y. You, Z. Huang, A. Umar, Y.S. Ibrahim, H. Algadi, L. Castañeda, H.A. Colorado, Corncob-derived activated carbon for efficient adsorption dye in sewage, ES Food Agrofor., 4 (2021) 61–73.
[15] H. Sudrajat, A. Susanti, D.K.Y. Putri, S. Hartuti, Mechanistic insights into the adsorption of methylene blue by particulate durian peel waste in water, Water Sci. Technol., 84 (2021) 1774–1792.
[16] X. Ma, Y. Liu, Q. Zhang, S. Sun, X. Zhou, Y. Xu, A novel natural lignocellulosic biosorbent of sunflower stem-pith for textile cationic dyes adsorption, J. Cleaner Prod., 331 (2021) 129878, doi: 10.1016/j.jclepro.2021.129878.
[17] S.H. Paiman, M.A. Rahman, T. Uchikoshi, N. Abdullah, M.H.D. Othman, J. Jaafar, K.H. Abas, A.F. Ismail, Functionalization effect of Fe-type MOF for methylene blue adsorption, J. Saudi Chem. Soc., 24 (2020) 896–905.
[18] M. Nazaripour, M.A.M. Reshadi, S.A. Mirbagheri, M. Nazaripour, A. Bazargan, Research trends of heavy metal removal from aqueous environments, J. Environ. Manage., 287 (2021) 112322, doi: 10.1016/j.jenvman.2021.112322.
[19] B. Qiu, X. Tao, H. Wang, W. Li, X. Ding, H. Chu, Biochar as a low-cost adsorbent for aqueous heavy metal removal: a review, J. Anal. Appl. Pyrolysis, 155 (2021) 105081, doi: 10.1016/j.jaap.2021.105081.
[20] M. Yadav, G. Singh, R.N. Jadeja, Physical and Chemical Methods for Heavy Metal Removal, P. Singh, R. Singh, V. Kumar Singh, R. Bhadouria, Eds., Pollutants and Water Management: Resources, Strategies and Scarcity, 2021, pp. 377–397.
[21] U.W.R. Siagian, K. Khoiruddin, A.K. Wardani, P.T.P. Aryanti, I. Nyoman Widiasa, G. Qiu, Y.P. Ting, I. Gede Wenten, High-performance ultrafiltration membrane: recent progress and its application for wastewater treatment, Curr. Pollut. Rep., 7 (2021) 448–462, doi: 10.1007/s40726-021-00204-5.
[22] S. Xue, Y. Xiao, G. Wang, J. Fan, K. Wan, Q. He, M. Gao, Z. Miao, Adsorption of heavy metals in water by modifying $Fe_3O_4$ nanoparticles with oxidized humic acid, Colloids Surf., A, 616 (2021) 126333, doi: 10.1016/j.colsurfa.2021.126333.
[23] M. Kanoje, M. Bhor, S. Toche, P. Jadhav, Removal of zinc from industrial wastewater using rice husk and activated carbon, Int. Res. J. Eng. Technol., 8 (2021) 2188–2190.
[24] N.A.A. Qasem, R.H. Mohammed, D.U. Lawal, Removal of heavy metal ions from wastewater: a comprehensive and critical review, npj Clean Water, 4 (2021) 1–15, doi: 10.1038/s41545-021-00127-0.
[25] M.S. Manna, C. Bhaumik, Opportunities and Challenges, Inamuddin, M.I. Ahamed, E. Lichtfouse, T. Altalhi, Eds., Remediation of Heavy Metals. Environmental Chemistry for a Sustainable World, Vol. 70, Springer, Cham, 2021, pp. 347–366.
[26] A. Tripathi, M.R. Ranjan, Heavy metal removal from wastewater using low cost adsorbents, J. Biorem. Biodegrad., 6 (2015) 315.
[27] Z. Zhang, T. Wang, H. Zhang, Y. Liu, B. Xing, Adsorption of Pb(II) and Cd(II) by magnetic activated carbon and its mechanism, Sci. Total Environ., 757 (2021) 143910, doi: 10.1016/j.scitotenv.2020.143910.
[28] D.R. Lobato-Peralta, E. Duque-Brito, A. Ayala-Cortés, D.M. Arias, A. Longoria, A.K. Cuentas-Gallegos, P.J. Sebastian, P.U. Okoye, Advances in activated carbon modification, surface heteroatom configuration, reactor strategies, and regeneration methods for enhanced wastewater treatment, J. Environ. Chem. Eng., 9 (2021) 105626, doi: 10.1016/j.jece.2021.105626.
[29] H. Yi, K. Nakabayashi, S.-H. Yoon, J. Miyawaki, Pressurized physical activation: a simple production method for activated carbon with a highly developed pore structure, Carbon, 183 (2021) 735–742.
[30] J. Nyirenda, K. Zombe, G. Kalaba, C. Siabbamba, I. Mukela, Exhaustive valorization of cashew nut shell waste as a potential bioresource material, Sci. Rep., 11 (2021) 1–14, doi: 10.1038/s41598-021-91571-y.
[31] G. Kaur, N. Singh, A. Rajor, Adsorption of doxycycline hydrochloride onto powdered activated carbon synthesized

from pumpkin seed shell by microwave-assisted pyrolysis, Environ. Technol. Innovation, 23 (2021) 101601, doi: 10.1016/j.eti.2021.101601.
[32] E.R. Raut, A.B. Thakur, A.R. Chaudhari, Review on toxic metal ions removal by using activated carbon prepared from natural biomaterials, J. Phys. Conf. Ser., 1913 (2021) 012091.
[33] Y. Gokce, S. Yaglikci, E. Yagmur, A. Banford, Z. Aktas, Adsorption behaviour of high performance activated carbon from demineralised low rank coal (Rawdon) for methylene blue and phenol, J. Environ. Chem. Eng., 9 (2021) 104819, doi: 10.1016/j.jece.2020.104819.
[34] M. Om Prakash, G. Raghavendra, S. Ojha, M. Panchal, Characterization of porous activated carbon prepared from arhar stalks by single step chemical activation method, Mater. Today: Proc., 39 (2021) 1476–1481.
[35] L. Pandey, S. Sarkar, A. Arya, A.L. Sharma, A. Panwar, R.K. Kotnala, A. Gaur, Fabrication of activated carbon electrodes derived from peanut shell for high-performance supercapacitors, Biomass Convers. Biorefin., (2021) 1–10, doi: 10.1007/s13399-021-01701-9.
[36] P. Senthil Kumar, S. Ramalingam, R.V. Abhinaya, K.V. Thiruvengadaravi, P. Baskaralingam, S. Sivanesan, Lead(II) adsorption onto sulphuric acid treated cashew nut shell, Sep. Sci. Technol., 46 (2011) 2436–2449.
[37] A.M. Alkherraz, A.K. Ali, K.M. Elsherif, Removal of Pb(II), Zn(II), Cu(II) and Cd(II) from aqueous solutions by adsorption onto olive branches activated carbon: equilibrium and thermodynamic studies, Chem. Int., 6 (2020) 11–20.
[38] Z.M. Yunus, A. Al-Gheethi, N. Othman, R. Hamdan, N.N. Ruslan, Removal of heavy metals from mining effluents in tile and electroplating industries using honeydew peel activated carbon: a microstructure and techno-economic analysis, J. Cleaner Prod., 251 (2020) 119738, doi: 10.1016/j.jclepro.2019.119738.
[39] V. Nejadshafiee, M.R. Islami, Intelligent-activated carbon prepared from pistachio shells precursor for effective adsorption of heavy metals from industrial waste of copper mine, Environ. Sci. Pollut. Res., 27 (2020) 1625–1639.
[40] V. Nejadshafiee, M.R. Islami, Bioadsorbent from magnetic activated carbon hybrid for removal of dye and pesticide, ChemistrySelect, 5 (2020) 8814–8822.
[41] T.M. Alslaibi, I. Abustan, M.A. Ahmad, A.A. Foul, Kinetics and equilibrium adsorption of iron(II), lead(II), and copper(II) onto activated carbon prepared from olive stone waste, Desal. Water Treat., 52 (2014) 7887–7897.
[42] R. Srivastava, D.C. Rupainwar, A comparative evaluation for adsorption of dye on Neem bark and Mango bark powder, Indian J. Chem. Technol., 18 (2011) 67–75.
[43] A.R. Kaveeshwar, S.K. Ponnusamy, E.D. Revellame, D.D. Gang, M.E. Zappi, R. Subramaniam, Pecan shell based activated carbon for removal of iron(II) from fracking wastewater: adsorption kinetics, isotherm and thermodynamic studies, Process Saf. Environ. Prot., 114 (2018) 107–122.
[44] P. Mishra, K. Singh, U. Dixit, Adsorption, kinetics and thermodynamics of phenol removal by ultrasound-assisted sulfuric acid-treated pea (*Pisum sativum*) shells, Sustainable Chem. Pharm., 22 (2021) 100491, doi: 10.1016/j.scp.2021.100491.
[45] J.S. Piccin, G. Dotto, L.A.A. Pinto, Adsorption isotherms and thermochemical data of FDandC Red N° 40 binding by chitosan, Braz. J. Chem. Eng., 28 (2011) 295–304.
[46] O. Üner, Ü. Geçgel, Y. Bayrak, Adsorption of methylene blue by an efficient activated carbon prepared from *Citrullus lanatus* rind: kinetic, isotherm, thermodynamic, and mechanism analysis, Water, Air, Soil Pollut., 227 (2016) 1–15, doi: 10.1007/s11270-016-2949-1.
[47] M.S. Abdelbassit, K.R. Alhooshani, T.A. Saleh, Silica nanoparticles loaded on activated carbon for simultaneous removal of dichloromethane, trichloromethane, and carbon tetrachloride, Adv. Powder Technol., 27 (2016) 1719–1729.
[48] M.S. Santana, R.P. Alves, L.S. Santana, M.A. Gonçalves, M.C. Guerreiro, Structural, inorganic, and adsorptive properties of hydrochars obtained by hydrothermal carbonization of coffee waste, J. Environ. Manage., 302 (2022) 114021, doi: 10.1016/j.jenvman.2021.114021.
[49] Darmadi, Mahidin, S.S. Azzahra, M. Masrura, Adsorption of mercury(II) ion in aqueous solution by using bentonite-based monolith, Key Eng. Mater., 885 (2021) 77–84.
[50] M.N. Alnajrani, O.A. Alsager, Removal of antibiotics from water by polymer of intrinsic microporosity: isotherms, kinetics, thermodynamics, and adsorption mechanism, Sci. Rep., 10 (2020) 1–14, doi: 10.1038/s41598-020-57616-4.
[51] A.N. Kani, E. Dovi, F.M. Mpatani, Z. Li, R. Han, L. Qu, Tiger nut residue as a renewable adsorbent for methylene blue removal from solution: adsorption kinetics, isotherm, and thermodynamic studies, Desal. Water Treat., 191 (2020) 426–437.
[52] K.H. Karim, Copper adsorption behavior in some calcareous soils using Langmuir, Freundlich, Temkin, and Dubinin–Radushkevich models, J. Soil Sci. Agric. Eng., 11 (2020) 27–34.
[53] P.M. Sanka, M.J. Rwiza, K.M. Mtei, Removal of selected heavy metal ions from industrial wastewater using rice and corn husk biochar, Water, Air, Soil Pollut., 231 (2020) 1–13, doi: 10.1007/s11270-020-04624-9.
[54] R. Gupta, S.K. Gupta, D.D. Pathak, Selective adsorption of toxic heavy metal ions using guanine-functionalized mesoporous silica [SBA-16-g] from aqueous solution, Microporous Mesoporous Mater., 288 (2019) 109577, doi: 10.1016/j.micromeso.2019.109577.
[55] B. Meroufel, O. Benali, M. Benyahia, Y. Benmoussa, M. Zenasni, Adsorptive removal of anionic dye from aqueous solutions by Algerian kaolin: characteristics, isotherm, kinetic and thermodynamic studies, J. Mater. Environ. Sci., 4 (2013) 482–491.
[56] N. Vučković, M. Nikodijević, D. Đorđević, The study of direct dye sorption on flax fibers during dyeing, Chem. Ind. Chem. Eng. Q., 27 (2021) 255–263.
[57] R. Ediati, M.A. Setyani, D.O. Sulistiono, E. Santoso, D. Hartanto, M.M.A.B. Abdullah, Optimization of the use of mother liquor in the synthesis of HKUST-1 and their performance for removal of chromium(VI) in aqueous solutions, J. Water Process Eng., 39 (2021) 101670, doi: 10.1016/j.jwpe.2020.101670.
[58] M.E. González-López, C.M. Laureano-Anzaldo, A.A. Pérez-Fonseca, M. Arellano, J.R. Robledo-Ortíz, A critical overview of adsorption models linearization: methodological and statistical inconsistencies, Sep. Purif. Rev., (2021) 1–15, doi: 10.1080/15422119.2021.1951757.
[59] G.K. Rajahmundry, C. Garlapati, P.S. Kumar, R.S. Alwi, D.-V.N. Vo, Statistical analysis of adsorption isotherm models and its appropriate selection, Chemosphere, 276 (2021) 130176, doi: 10.1016/j.chemosphere.2021.130176.
[60] A. Agarwal, M. Rastogi, N.B. Singh, Agricultural Wastes Utilization in Water Purification, in: Inorganic-Organic Composites for Water and Wastewater Treatment, Vol. 1, Springer, Hong Kong, 2022, pp. 147–168.
[61] M. Sadani, T. Rasolevandi, H. Azarpira, A.H. Mahvi, M. Ghaderpoori, S.M. Mohseni, A. Atamaleki, Arsenic selective adsorption using a nanomagnetic ion imprinted polymer: optimization, equilibrium, and regeneration studies, J. Mol. Liq., 317 (2020) 114246, doi: 10.1016/j.molliq.2020.114246.
[62] K.A.M. Said, N.Z. Ismail, R.L. Jama'in, N.A.M. Alipah, N.M. Sutan, G.G. Gadung, R. Baini, N.S.A. Zauzi, Application of Freundlich and Temkin isotherm to study the removal of Pb(II) via adsorption on activated carbon equipped polysulfone membrane, Int. J. Eng. Technol., 7 (2018) 91–93.
[63] S. Tan, K. Saito, M.T.W. Hearn, Isothermal modelling of protein adsorption to thermo-responsive polymer grafted Sepharose Fast Flow sorbents, J. Sep. Sci., 44 (2021) 1884–1892.
[64] K. Nuithitikul, R. Phromrak, W. Saengngoen, Utilization of chemically treated cashew-nut shell as potential adsorbent for removal of Pb(II) ions from aqueous solution, Sci. Rep., 10 (2020) 1–14, doi: 10.1038/s41598-020-60161-9.
[65] K.P.D.A. N'goran, D. Diabaté, K.M. Yao, N.L.B. Kouassi, U.P. Gnonsoro, K.C. Kinimo, A. Trokourey, Lead and cadmium removal from natural freshwater using mixed activated carbons from cashew and shea nut shells, Arabian J. Geosci., 11 (2018) 1–12, doi: 10.1007/s12517-018-3862-2.
[66] V. Manirethan, R.M. Balakrishnan, Batch and continuous studies on the removal of heavy metals using biosynthesised melanin

impregnated activated carbon, Environ. Technol. Innovation, 20 (2020) 101085, doi: 10.1016/j.eti.2020.101085.
[67] R. Shahrokhi-Shahraki, C. Benally, M.G. El-Din, J. Park, High efficiency removal of heavy metals using tire-derived activated carbon vs commercial activated carbon: insights into the adsorption mechanisms, Chemosphere, 264 (2021) 128455, doi: 10.1016/j.chemosphere.2020.128455.
[68] G.K.R. Angaru, Y.-L. Choi, L.P. Lingamdinne, J.-S. Choi, D.-S. Kim, J.R. Koduru, J.-K. Yang, Y.-Y. Chang, Facile synthesis of economical feasible fly ash–based zeolite–supported nano zerovalent iron and nickel bimetallic composite for the potential removal of heavy metals from industrial effluents, Chemosphere, 267 (2021) 128889, doi: 10.1016/j.chemosphere.2020.128889.
[69] E.K. Leizou, M.A. Ashraf, A.J.K. Chowdhury, H. Rashid, Adsorption studies of $Pb^{2+}$ and $Mn^{2+}$ ions on low-cost adsorbent: unripe plantain (*Musa paradisiaca*) peel biomass, Acta Chem. Malaysia (ACMY), 2 (2018) 11–15.
[70] K. Sudha Rani, B. Srinivas, K. GouruNaidu, K.V. Ramesh, Removal of copper by adsorption on treated laterite, Mater. Today: Proc., 5 (2018) 463–469.
[71] H. Sivasankari, K. Ramesh, A. Rajappa, Influence of acid and base surface modification on Cr(VI) ions adsorption onto activated carbons prepared from bark of *Thespesia populnea*-isotherm and thermodynamics study, J. Adv. Sci. Res., 12 (2021) 314–324.
[72] M. Shafiq, A. Alazba, M.T. Amin, Removal of heavy metals from wastewater using date palm as a biosorbent: a comparative review, Sains Malaysiana, 47 (2018) 35–49.
[73] U. Maheshwari, Removal of Metal Ions From Wastewater Using Adsorption: Experimental and Theoretical Studies, Birla Institute of Technology and Science, Pilani, Thesis, 2015.
[74] M.U. Tahir, X. Su, M. Zhao, Y. Liao, R. Wu, D. Chen, Preparation of hydroxypropyl-cyclodextrin-graphene/$Fe_3O_4$ and its adsorption properties for heavy metals, Surf. Interfaces, 16 (2019) 43–49.
[75] L. Dong, L. Hou, Z. Wang, P. Gu, G. Chen, R. Jiang, A new function of spent activated carbon in BAC process: removing heavy metals by ion exchange mechanism, J. Hazard. Mater., 359 (2018) 76–84.
[76] K.H. Chu, Revisiting the Temkin isotherm: dimensional inconsistency and approximate forms, Ind. Eng. Chem. Res., 60 (2021) 13140–13147.
[77] E. Ernest, O. Onyeka, C.M. Aburu, C.C. Aniobi, J.O. Ndubuisi, Adsorption efficiency of activated carbon produced from corn cob for the removal of cadmium ions from aqueous solution, Acad. J. Chem., 4 (2019) 12–20.
[78] S. Abdulrazak, K. Hussaini, H.M. Sani, Evaluation of removal efficiency of heavy metals by low-cost activated carbon prepared from African palm fruit, Appl. Water Sci., 7 (2017) 3151–3155.
[79] T. Van Tran, Q.T.P. Bui, T.D. Nguyen, N.T.H. Le, L.G. Bach, A comparative study on the removal efficiency of metal ions ($Cu^{2+}$, $Ni^{2+}$, and $Pb^{2+}$) using sugarcane bagasse-derived $ZnCl_2$-activated carbon by the response surface methodology, Adsorpt. Sci. Technol., 35 (2017) 72–85.
[80] S. Ayub, A.A. Mohammadi, M. Yousefi, F. Changani, Performance evaluation of agro-based adsorbents for the removal of cadmium from wastewater, Desal. Water Treat., 142 (2019) 293–299.
[81] S. Saputro, L. Mahardiani, M. Masykuri, A.Z. Jazuli, The effectiveness of the activated carbon from coconut shell and corn cob to adsorb Pb(II) ion and it's analysis using solid-phase spectrophotometry, IOP Conf. Ser.: Mater. Sci. Eng., 578 (2019) 012020.
[82] A.H. Jawad, S.A. Mohammed, M.S. Mastuli, M.F. Abdullah, Carbonization of corn (*Zea mays*) cob agricultural residue by one-step activation with sulfuric acid for methylene blue adsorption, Desal. Water Treat., 118 (2018) 342–351.
[83] C. Yu, H. Wang, M. Lu, F. Zhu, Y. Yang, H. Huang, C. Zou, J. Xiong, Z. Zhong, Application of rice straw, corn cob, and lotus leaf as agricultural waste derived catalysts for low temperature SCR process: optimization of preparation process, catalytic activity and characterization, Aerosol Air Qual. Res., 20 (2020) 862–876.
[84] A.H. Jawad, A.S. Abdulhameed, M.S. Mastuli, Acid-factionalized biomass material for methylene blue dye removal: a comprehensive adsorption and mechanism study, J. Taibah Univ. Sci., 14 (2020) 305–313.
[85] U. Farooq, M.A. Khan, M. Athar, J.A. Kozinski, Effect of modification of environmentally friendly biosorbent wheat (*Triticum aestivum*) on the biosorptive removal of cadmium(II) ions from aqueous solution, Chem. Eng. J., 171 (2011) 400–410.
[86] M.O. Bello, N. Abdus-Salam, F.A. Adekola, U. Pal, Isotherm and kinetic studies of adsorption of methylene blue using activated carbon from ackee apple pods, Chem. Data Collect., 31 (2021) 100607, doi: 10.1016/j.cdc.2020.100607.
[87] M.A. Ahmad, M.A. Eusoff, P.O. Oladoye, K.A. Adegoke, O.S. Bello, Optimization and batch studies on adsorption of Methylene blue dye using pomegranate fruit peel based adsorbent, Chem. Data Collect., 32 (2021) 100676, doi: 10.1016/j.cdc.2021.100676.
[88] C. Zou, W. Jiang, J. Liang, X. Sun, Y. Guan, Removal of Pb(II) from aqueous solutions by adsorption on magnetic bentonite, Environ. Sci. Pollut. Res., 26 (2019) 1315–1322.
[89] S. Tahazadeh, T. Mohammadi, M.A. Tofighy, S. Khanlari, H. Karimi, H.B.M. Emrooz, Development of cellulose acetate/metal-organic framework derived porous carbon adsorptive membrane for dye removal applications, J. Membr. Sci., 638 (2021) 119692, doi: 10.1016/j.memsci.2021.119692.
[90] K.L. Yu, X.J. Lee, H.C. Ong, W.-H. Chen, J.-S. Chang, C.-S. Lin, P.L. Show, T.C. Ling, Adsorptive removal of cationic methylene blue and anionic Congo red dyes using wet-torrefied microalgal biochar: equilibrium, kinetic and mechanism modeling, Environ. Pollut., 272 (2021) 115986, doi: 10.1016/j.envpol.2020.115986.
[91] D. Obregón-Valencia, M. del Rosario Sun-Kou, Comparative cadmium adsorption study on activated carbon prepared from aguaje (*Mauritia flexuosa*) and olive fruit stones (*Olea europaea* L.), J. Environ. Chem. Eng., 2 (2014) 2280–2288.
[92] K.-Y. Shin, J.-Y. Hong, J. Jang, Heavy metal ion adsorption behavior in nitrogen-doped magnetic carbon nanoparticles: isotherms and kinetic study, J. Hazard. Mater., 190 (2011) 36–44.
[93] Y. Miyah, A. Lahrichi, M. Idrissi, Removal of cationic dye–methylene blue–from aqueous solution by adsorption onto corn cob powder calcined, J. Mater. Environ. Sci., 7 (2016) 96–104.
[94] P.M.K. Reddy, P. Verma, C. Subrahmanyam, Bio-waste derived adsorbent material for methylene blue adsorption, J. Taiwan Inst. Chem. Eng., 58 (2016) 500–508.